Incorporation of Oval-Slot and Arc-Slits Upon Planar Oval Monopole Antenna for Radiation Characteristics Improvement

Agus D. Prasetyo[1,2]
[1]*Radio Telecommunication and Microwave Laboratory*
School of Electrical Engineering & Informatics, ITB
[2]*School of Electrical Engineering, Telkom University*
Bandung, Indonesia
33220316@std.stei.itb.ac.id

Deny Hamdani
School of Electrical Engineering & Informatics
Institut Teknologi Bandung
Bandung, Indonesia
deny@power.ee.itb.ac.id

Budi Syihabuddin[1,2]
[1]*Radio Telecommunication and Microwave Laboratory*
School of Electrical Engineering & Informatics, ITB
[2]*School of Electrical Engineering, Telkom University*
Bandung, Indonesia
budisyihab@telkomuniversity.ac.id

Achmad Munir
Radio Telecommunication and Microwave Laboratory
School of Electrical Engineering & Informatics
Institut Teknologi Bandung
Bandung, Indonesia
munir@ieee.org

***Abstract*—This paper proposes the improvement of planar oval monopole antenna radiation characteristics by incorporating an oval-slot and arc-slits upon its radiating patch. The oval shape of the patch was obtained theoretically by determining a triangle-to-oval formula. A modification on the radiating patch by involving an oval slot geometrically scaled down from its dimensions is proposed to enhance the radiation characteristics. Moreover, two pairs of arc slits are also embedded into the patch for the enhancement. The modification stage is carried out through simulations in which experimental characterizations are used to validate the final configuration. The characterization is performed in an anechoic chamber in the frequency range of 1–20 GHz. The characterization results show that the incorporation of oval-slot and arc-slits into the radiating patch produces a reflection coefficient (S_{11}) of around 34.78% for S_{11} value between –10 dB to –20 dB. The proposed antenna configuration works at the frequency band of 1.38–20 GHz with two rejection bands of around the frequency ranges of 1.95–3.47 GHz and 9.08–9.55 GHz. The radiation patterns are measured at the frequencies of 5.66 GHz, 8.03 GHz, and 13.54 GHz to analyze the effect of improvement due to the modification. Furthermore, investigations on the distribution of surface current are also performed to determine the potency of modification offered for future developments.**

***Index Terms*—arc-slits; planar oval monopole antenna; oval-slot; radiation characteristics.**

I. Introduction

In the last decade, research on techniques for bandwidth widening of planar monopole antennas and improving characteristics performance is still becoming a hot issue in the antenna development of wideband or ultra-wideband (UWB) and other broadband antenna topics. Many researchers have investigated several techniques used in their reports [1]–[11]. Some of them applied unique techniques to the antenna structure using slot, slit, and fractal approach [1]–[3]. The use of slots and/or slits with specific configurations upon the radiating patch of antenna was one of the techniques which affect the bandwidth response and radiation characteristic [1]–[2]. The combination of oval-shaped slots and a pair of slits incorporated into a planar monopole patch antenna was introduced [2]. This research has proposed two types of slits, namely rectangular slits and semi-circular slits. The configurations which use semi-circular slits could provide better bandwidth response than the rectangular ones at the frequency range of 2.96–18 GHz.

The rectangular path slits have also been incorporated into radiating patch and groundplane [4], so that the antenna worked at the frequency band of 3.02–13.86 GHz with two rejection bands of around the frequency ranges of 3.38–4.31 GHz and 5.1–5.95 GHz. It is inferred that the role of slit was also identified to enhance the characteristics, as well as the performance of antenna. In [5], a cross-shaped slit was suggested to be engraved on a planar monopole antenna with a circular patch. However, in the frequency range of 2–7 GHz, the use of cross-slit was unsatisfactory as it causes a deterioration in its performance. Meanwhile, the exploration on slits and slots for UWB antennas has been reported [6]. In fact, the overall configuration was similar to what was carried out in [4], however there was a groundplane involved in the design. The bandwidth response of the configuration was at the frequency range of 2.89–17.83 GHz with two rejection bands of around the frequency ranges of 3.47–4.33 GHz and 5.11–5.94 GHz.

In line with the effect of adding rectangular slits on the planar monopole of the antenna, the works reported in [7]–[9] have shown that pairs of slits attached to the sides of the radiating patch could exert a constructive influence, in this case the reflection coefficient (S_{11}) performance, with proper consideration. The use of large slots on planar monopole antennas with oval shape of patches has also been proposed [10]. Despite unusual configuration regarding the connection between the patch and the groundplane, the proposed antenna was capable to operate at the UWB range. Furthermore, the involvements of egg-like or oval shape of patch have also been explored [11]–[14]. In [11]–[12], a spline interpolation of three vertices of an isosceles triangle was used to form an egg-like or oval shape. Meanwhile, a mathematical approach has been implemented to determine the degree of patch ovality [13]–[14]. These four configurations were reported to cover UWB applications.

This paper proposes the improvement of radiation characteristics for a planar oval monopole antenna by incorporating an oval-slot and a pair of arc-slits upon its radiating patch. In the previous achievement [14], the value of S_{11} in the frequency range of 10–15 GHz was dominated by the range values of –10 dB to –15 dB. To simplify the slot shape, a geometrically scaled down of the radiating patch of the planar oval monopole antenna is used. The proposed pair of slits used for the enhancement takes the form of an arc. Several attempts to improve the characteristics performance by varying each parameter used for oval-slot and arc-slits will be described. Radiation characteristics of the proposed antenna, i.e., S_{11}, will be compared with the previous achievement. The measured radiation patterns will also be presented and discussed. In addition, a simulation investigation is carried out to observe the changes in the surface current distribution for the modified radiating patch.

II. Antenna Configuration

The proposed antenna is designed on a 49.6 mm × 39 mm × 1.57 mm size RT/duroid 5880, which has the relative permittivity of 2.2 and the dielectric loss of 0.0009. As illustrated in Fig. 1, there are two configurations of antenna model used for the investigation. The first model, i.e., Model I, is the original configuration used as a reference [14], and the second one, i.e., Model II, is a proposed configuration with the addition of oval-slot and two pairs of arc-slits. Both models use the same oval patch which was obtained from a triangle-to-oval geometry using k = 0.06 and equipped with an identical feeding line and a partial groundplane [14]. The radiating patch on Model II is featured by an oval-slot built from the scaled down patch and placed concentrically upon the radiating patch. Two pairs of arc-slits are arranged in such a way in which each arc-slit has the arc radius of r_1 and r_2, the arc angle of a_1 and a_2, and the slit width of w_1 and w_2, respectively.

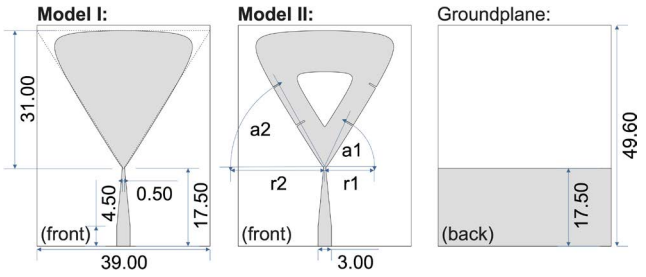

Fig. 1. Antenna configurations for Model I and Model II (dimensions are in millimeter (mm) unit).

The measured result of Model I, obtained from the previous achievement [14], is used as a reference for how much the radiation characteristics can be enhanced. To determine the scale of an oval slot, simulations are carried out by varying the scaling down value. Fig. 2 plots the results of 30%, 40%, and 50% scaling values compared to the measured results of Model I. These results show that the

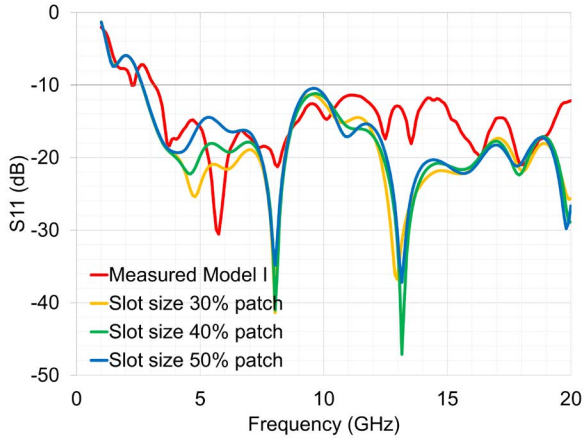

Fig. 2. Comparison of S_{11} value between measured result of Model I and simulated result of proposed antenna with varied slot size.

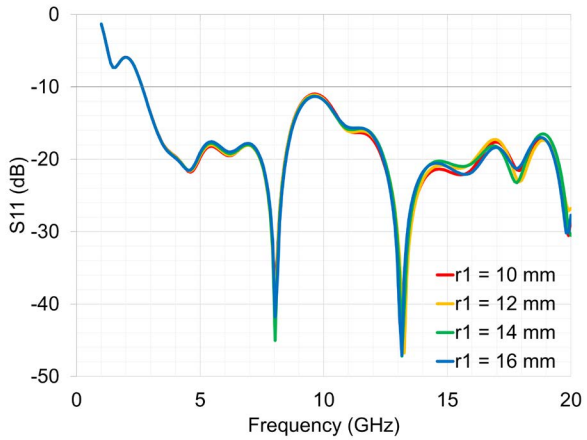

Fig. 3. Comparison of S_{11} value for proposed antenna with varied radius of first arc-slits pair (r_1).

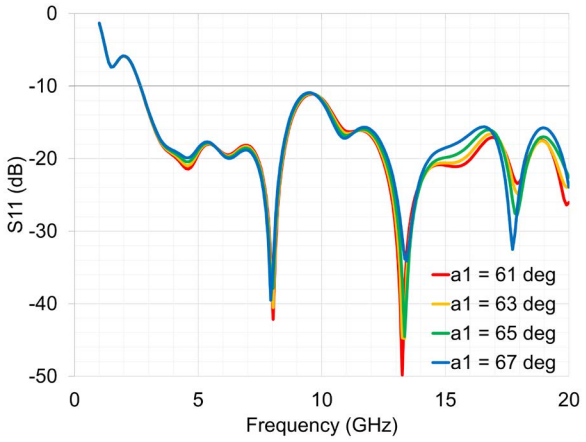

Fig. 4. Comparison of S_{11} value for proposed antenna with varied angle of first arc slits pair (a_1).

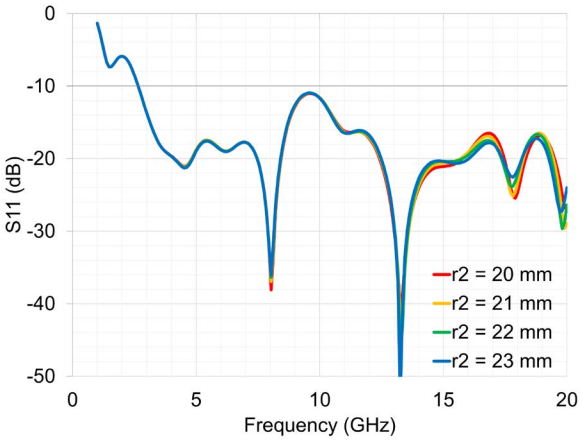

Fig. 6. Comparison of S_{11} value for proposed antenna with varied radius of second arc-slits pair (r_2).

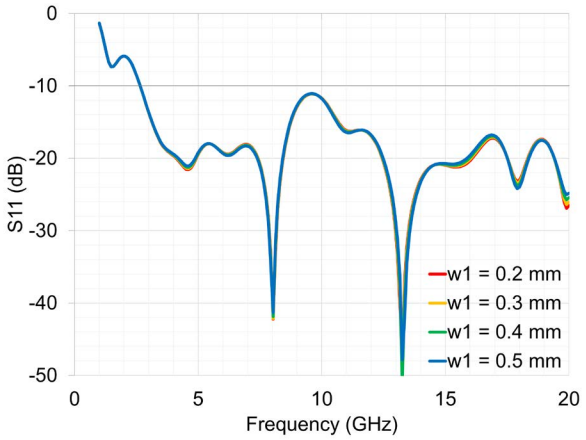

Fig. 5. Comparison of S_{11} value for proposed antenna with varied width of first arc-slits pair (w_1).

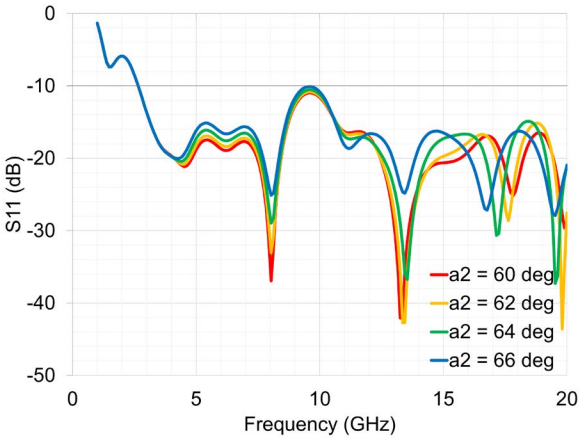

Fig. 7. Comparison of S_{11} value for proposed antenna with varied angle of second arc-slits pair (a_2).

required scaling value to create the oval-slot incorporated into the radiating patch of the planar oval monopole antenna is 40%. The same approach is also used to determine the radius of the first arc-slits (r_1). The alterations are carried out by observing changes in the response of S_{11} to r_1 at the values of 10, 12, 14, and 16 mm. The simulated results are depicted in Fig. 3, whereby the r_1 value of 12 mm is chosen. This value is based on the S_{11} value in the frequency range of 10–15 GHz, which is better than the other ones.

As shown in Fig. 4, the variation of a_1 value is simulated with a magnitude of 61°, 63°, 65°, and 67°. The a_1 value of 61° is taken as it has a minimum S_{11} value at the frequency of 13.26 GHz, which is –49.84 dB, lower than the others. The next characterization is performed by changing the value of w_1, where the results are plotted in Fig. 5. It shows that a slight change of w_1 insignificantly affects the S_{11} value. Here, the consideration is taken for the accuracy of antenna fabrication, so 0.3 mm is chosen as the value of w_1.

The characterization also applies for various radius values of the second arc-slits. From the results shown in Fig. 6, by taking into account a balanced performance of S_{11} value, the value of r_2 is 21 mm. Furthermore, the simulated results for varied value of a_2 is depicted in Fig. 7. From the previous result in varying a_1 values at 60°, 62°, 64°, and 66°, there are more visible changes in determining the value of a_1. Some minima that approach or exceed –30 dB appeared, especially at the a_2 value of 64°, occur at the frequencies of 8.03 GHz, 13.54 GHz, 17.25 GHz, and 19.53 GHz.

The results show that the oval-slot has a dominant effect on the S_{11} value at the frequency range below 8 GHz, although there is a slight change in other frequency ranges. By using a 40% scaling value, the proposed antenna is advantageous to the characteristics as it also produces preferable S_{11} values at the frequencies of 8.03 GHz and 13.16 GHz. The minor changes in the S_{11} value occur when the w_1 value changes. By changing the radius of arc-slits for both radiuses, i.e., r_1

and r_2, fluctuations in the S_{11} value are more likely to be at the minima previously obtained in the frequency ranges above 14 GHz. The most dominant change in the S_{11} value which apart from the change in oval-slot size occurs when the arc-slit angles are changed.

III. Results and Discussion

Based on the results explained in the previous section, the proposed antenna is fabricated and experimentally characterized in an anechoic chamber, as depicted in Fig. 8. The comparison of S_{11} value between the measured result for Model I and Model II and the simulated result for Model II is plotted in Fig. 9. The results show some discrepancies between the simulation and the measurement. These discrepancies occurred as the simulation was performed at a constant value of relative permittivity and dielectric loss. However, the pattern of the S_{11} value remains well predictable. The measured result for Model I has a very wide single-band from the frequency of 3.06 GHz to 20 GHz. Whilst the measured result for Model II works at the frequency range of 1.38–20 GHz with two rejection bands of around the frequency ranges of 1.95–3.47 GHz and 9.08–9.55 GHz.

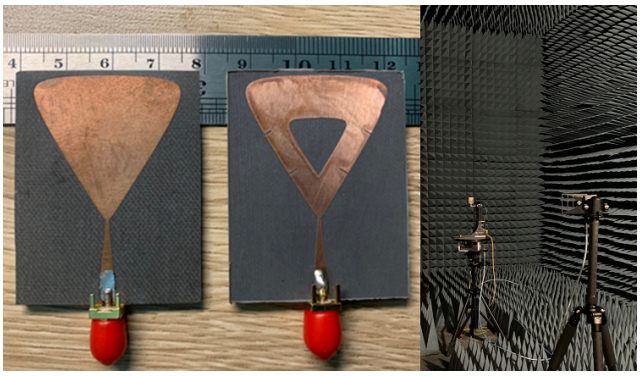

Fig. 8. Photograph of fabricated antennas for Model I (left) and Model II (right), and its experimental characterization setup in an anechoic chamber.

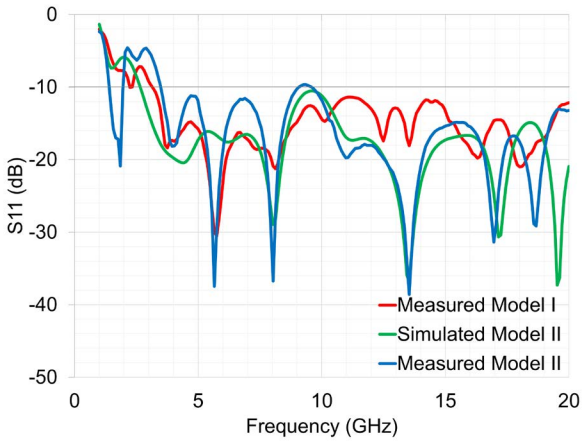

Fig. 9. Comparison of S_{11} value between antenna Model I and Model II.

Furthermore, the measured results for Model I show that the minima which exceed –20 dB occur at the frequencies of 5.75 GHz, 8.13 GHz, and 18.10 GHz with the S_{11} values of –30.54 dB, –21.28 dB, and –20.92 dB, respectively. On the other hand, the measured results for Model II have a minimum S_{11} value that exceeds –20 dB at the frequencies of 1.86 GHz, 5.66 GHz, 8.03 GHz, 13.54 GHz, 16.96 GHz, and 18.67 GHz, which are –20.89 dB, –37.45 dB, –36.75 dB, –38.59 dB, –31.36 dB, and –29.15 dB, respectively. In Model I, the distribution of the minima, which has the S_{11} value less than –20 dB from the overall S_{11} value and less than –10 dB, is around 12.35%. Meanwhile, the distribution of the minima in Model II reached around 34.78%.

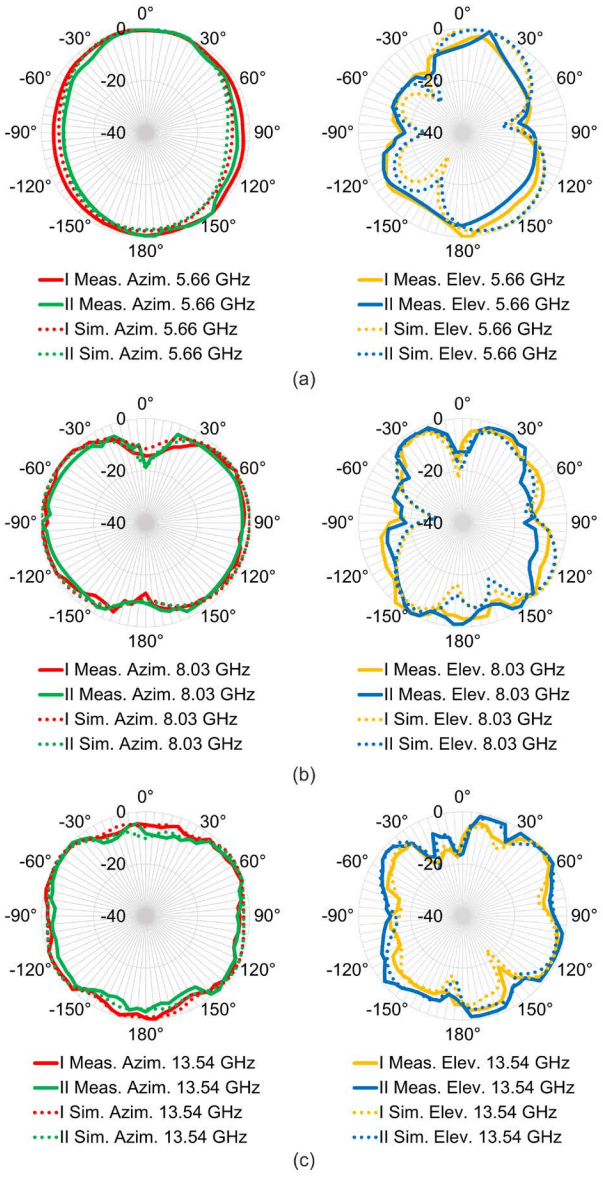

Fig. 10. Normalized measured radiation patterns for Model I and Model II at frequencies of (a) 5.66 GHz, (b) 8.03 GHz, and (c) 13.54 GHz, left is azimuth plane, and right is elevation plane.

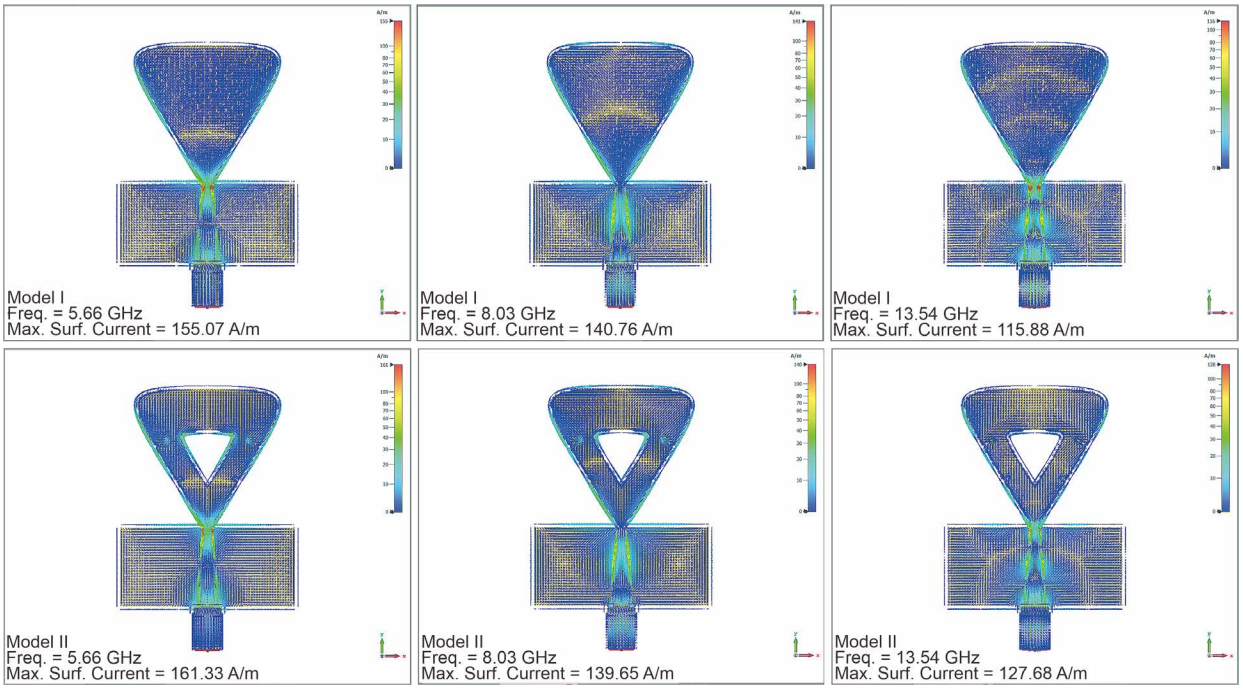

Fig. 11. Surface current distribution for Model I (top) and Model II (bottom) at frequencies of 5.66 GHz, 8.03 GHz, and 13.54 GHz.

Fig. 10 depicts the normalized measured radiation patterns for Model I and Model II in the azimuth and elevation planes taken at the frequencies of 5.66 GHz, 8.03 GHz, and 13.54 GHz. These frequencies were chosen as both models have nearly aligned the minima in their S_{11} values. The simulated radiation patterns for both models are also depicted together as comparison. It is seen that both models on the simulation and measurement results agreed well. Moreover, the main focus of discussion on the radiation patterns is to compare the measurement results for the two models.

As shown in Fig. 10 (a), Model I and Model II have the same maximum radiation orientation in the azimuth plane at the frequency of 5.66 GHz, which is at the angle of 140°. In the azimuth plane, the average of difference at each angle for Model I and Model II is 1.92 dB, with the maximum difference of 3.85 dB occurred at the angle of –125°. While in the elevation plane, the maximum radiation orientation for Model I and Model II is achieved at the angles of 175° and 15°, respectively. The average of difference from the measurement results at each angle is 1.62 dB with the maximum difference of 5.22 dB occurred at the angle of 175°. Thus, Model II can reduce the backlobe in the elevation plane at the angle of 175° and changes its maximum radiation orientation at the angle of 15°.

At the frequency of 8.03 GHz shown in Fig. 10 (b), a shift in the direction of maximum radiation occurs in the azimuth plane. Model I has the maximum radiation orientation at the angle of 60°, and at the angle of –90° for Model II. The average of difference between both models is 1.49 dB, and the maximum difference of 5.24 dB occurred at the angle of 20°. Meanwhile, at the elevation plane, there is also a shift in the direction of the maximum radiation orientation. Model I has the maximum radiation orientation at the angle of –140°, while Model II is at the angle of –150°. In the elevation plane, both models have the average of difference at each angle of 2.57 dB. The maximum radiation orientation at each angle is 7.80 dB which occurs at the angle of 5°.

Furthermore, at the frequency of 13.54 GHz shown in Fig. 10 (c), Model I produces the maximum radiation at the angle of 175° in the azimuth plane, while Model II is at the angle of 135°. The average of difference in radiation pattern between Model I and Model II is 1.69 dB, with the maximum difference of 5.50 dB occurred in the angle of –165°. In the elevation plane, the maximum radiation orientation for Model I and Model II are at the angles of 50° and 60°, respectively. Model I and Model II have the average of difference of 2.80 dB. The biggest difference occurs in the orientation of –20° which is 10.13 dB.

The investigation of surface current distribution on the proposed antenna is carried out through simulation. Fig. 11 depicts the investigation results at three frequencies used in the radiation pattern measurements, namely 5.66 GHz, 8.03 GHz, and 13.54 GHz for Model I and Model II. For Model I, the frequencies of 5.66 GHz, 8.03 GHz, and 13.54 GHz have maximum surface current values of 155.07 A/m, 140.76 A/m, and 115.88 A/m, respectively. Whilst for Model II, it produces maximum surface currents of 161.33 A/m, 139.65 A/m, and 127.68 A/m, respectively. It shows that the proposed antenna, i.e., Model II, slightly decreases by 1.11 A/m, in terms of its maximum surface current, at the

frequency of 8.03 GHz. However, at the frequencies of 5.66 GHz and 13.54 GHz, the surface current increases up to 6.26 A/m and 11.80 A/m, respectively. It can be inferred that the proposed modification yielded a significant improvements at those frequencies. Therefore, this technique is beneficial for further development to attain an improved characteristic on the overall working bandwidth.

In addition, the incorporation of two pairs of arc-slits on the radiating patch affects the overall capacitive properties of antenna. The incorporation also provides enhancement in the impedance matching. Whilst the addition of oval-slot positively contributes to the improvement of S_{11} response. In overall, the proposed modification affects in a more slender radiation pattern, except for the elevation plane at the frequency of 13.54 GHz, which means the proposed antenna has better directionality. From the observation of surface current distribution, the proposed modification also promises for further developments in the future, which can be explored to achieve an even better S_{11} response over the entire frequency ranges or to perform a desirable notch-band.

IV. Conclusion

The radiation characteristic improvement of planar oval monopole antenna by incorporating an oval-slot and two pairs of arc-slits upon its radiating patch has been presented. A series of processes performed on the proposed antenna, which was modified from the reference, i.e., Model I, showed that the incorporation of an oval-slot and two pairs of arc-slits upon the radiating patch of planar oval monopole antenna, i.e., Model II, has shown a significant improvement in the S_{11} value. Although there were rejection bands, the proposed modification has improved the radiation characteristics of antenna. The proposed modification has also enhanced the achievement of S_{11} response at the frequency range above 10 GHz. Meanwhile, the incorporation of an oval-slot and two pairs of arc-slits upon the radiating patch has provided a more directive radiation pattern at two of three selected frequencies, namely 5.66 GHz and 8.03 GHz. In addition, on the investigation of surface current distribution, Model II could significantly improve maximum surface current at the frequencies of 5.66 GHz and 13.54 GHz.

References

[1] A. Kurniawan and S. Mukhlishin, "Wideband and multiband antenna design and fabrication for modern wireless communications systems," *J. ICT Res. Appl.*, vol. 7, no. 2, pp. 151–163, Nov. 2013, DOI: 10.5614/itbj.ict.res.appl.2013.7.2.4.

[2] R. K. Parida, N. K. Sahoo, R. Swain, S. Swain, and D. C. Panda, "Comparative study of a novel UWB antenna for application in cognitive radio," in *Proc. International Conference on Applied Electromagnetics, Signal Processing and Communication (AESPC)*, Bhubaneswar, India, Oct. 2018, pp. 1–4, DOI: 10.1109/AESPC44649.2018.9033315.

[3] A. Munir, D. T. Putranto, and H. Wijanto, "Characterization of series iteration log-periodic fractal Koch printed antenna equipped with balun unit," *J. ICT Res. Appl.*, vol. 7, no. 3, pp. 191–204, Dec. 2013, DOI: 10.5614/itbj.ict.res.appl.2013.7.3.2.

[4] M. Ojaroudi, N. Ojaroudi, and N. Ghadimi, "Dual band-notched small monopole antenna with novel coupled inverted U-ring strip and novel fork-shaped slit for UWB applications," *IEEE Antennas Wireless Propag. Lett.*, Vol. 12, pp. 182–185, Feb. 2013, DOI: 10.1109/LAWP.2013.2245296.

[5] C. Liu, C. Chiu, and S. Deng, "A compact disc-slit monopole antenna for mobile devices," *IEEE Antennas Wireless Propag. Lett.*, Vol. 7, pp. 251–254, Mar. 2008, DOI: 10.1109/LAWP.2008.920751.

[6] M. Mehranpour, J. Nourinia, C. Ghobadi, and M. Ojaroudi, "Dual band-notched square monopole antenna for ultra-wideband applications," *IEEE Antennas Wireless Propag. Lett.*, Vol. 11, pp. 172–175, Feb. 2012, DOI: 10.1109/LAWP.2012.2186552.

[7] A. A. Kadam, A. A. Deshmukh, S. B. Deshmukh, A. Doshi, and K. P. Ray, "Slit loaded circular ultra wideband antenna for band notch characteristics," in *Proc. National Conference on Communications (NCC)*, Bangalore, India, Feb. 2019, pp. 1–6, DOI: 10.1109/NCC.2019.8732202.

[8] C. Guo, R. Yang, and W. Zhang, "Compact omnidirectional circularly polarized antenna loaded with complementary v-shaped slits," *IEEE Antennas Wireless Propag. Lett.*, Vol. 17, No. 9, pp. 1593–1597, Sep. 2018, DOI: 10.1109/LAWP.2018.2856504.

[9] J. Kulkarni, C.-Y.-D. Sim, R. K. Gangwar, and J. Anguera, "Broadband and compact circularly polarized MIMO antenna with concentric rings and oval slots for 5G application," *IEEE Access*, Vol. 10, pp. 29925–29936, Mar. 2022, DOI: 10.1109/ACCESS.2022.3157914.

[10] M. Tang and R. W. Ziolkowski, "Compact hyper-band printed slot antenna: Design and experiments," in *Proc. 8th European Conference on Antennas and Propagation (EuCAP)*, The Hague, Netherlands, Apr. 2014, pp. 594–596, DOI: 10.1109/EuCAP.2014.6901828.

[11] A. D. Prasetyo, B. S. Nugroho, B. Syihabuddin, and A. Munir, "Study on super wideband compact ovoidal printed antenna," in *PhotonIcs & Electromagnetics Research Symposium - Fall (PIERS - Fall)*, Xiamen, China, Dec. 2019, pp. 2235–2239, DOI: 10.1109/PIERS-Fall48861.2019.9021736.

[12] A. D. Prasetyo, D. Hamdani, and A. Munir, "Characterization of compact ovoidal printed antenna with windowed groundplane" in *Proc. International Workshop on Antenna Technology (iWAT)*, Dublin, Ireland, May 2022, pp. 176-179, DOI: 10.1109/iWAT54881.2022.9811080.

[13] S. Verma and P. Kumar, "Printed egg curved monopole antenna for ultrawideband applications," in *Proc. National Conference on Communications (NCC)*, New Delhi, India, Feb. 2013, pp. 1–5, DOI: 10.1109/NCC.2013.6487906.

[14] A. D. Prasetyo and A. Munir, "Bandwidth enhancement of wideb and sensor using triangle-to-oval patch geometric change for EMC measurement," in *Proc. Asia-Pacific International Symposium on Electromagnetic Compatibility (APEMC)*, Nusa Dua - Bali, Indonesia, Sep. 2021, pp. 1–4, DOI: 10.1109/APEMC49932.2021.9596731.